
Exposure-Adjusted Bicycle Crash Risk Estimation and Safer Routing in Berlin

Eric Berger * Edward Eichhorn * Liaisan Faidrakhmanova * Luise Grasl * Tobias Schnarr *

Abstract

We investigate bicycle crash risk on Berlin's urban street network, addressing a key limitation of many safety analyses: raw crash counts conflate danger with demand and fail to distinguish intrinsically risky locations from high-use roads. We combine police-reported crashes with a city-wide dataset of measured bicycle volumes to compute exposure-adjusted risk at the street-segment and junction levels. Aggregating risk to arbitrary routes enables comparisons that trade off safety against convenience. The result is a reproducible framework for exposure-controlled bicycle safety analysis and routing.

/edit, when we
nal results

cite source of official
bike counting stations

1. Introduction

Cycling safety analyses often rely on raw crash counts, which conflate danger with demand: streets with high cyclist volumes tend to accumulate more incidents even when per-rider risk is low (Lücke, 2018). This obscures intrinsically risky locations and limits both targeted interventions and everyday route choice, particularly in dense urban networks such as Berlin (Uijtdewilligen et al., 2024). We address this by estimating exposure-adjusted crash risk on the street network via a relative-risk formulation that separates cyclist demand from intrinsic danger and remains stable under sparse or unevenly distributed observations (Section 3). Using police-recorded crashes from the German *Accident Atlas* (Berlin subset) (German Federal Statistical Office, 2025) together with a city-wide dataset of measured bicycle volumes at the street-segment level (Kaiser, 2025), we estimate relative risk for individual street segments and, motivated by crash concentrations at intersections, derive junction-level risk by aggregating volumes from adjoining segments. These risk estimates are transformed into expected crash costs and propagated to route-level scores, enabling comparisons between shortest paths and safer alternatives that

reduce estimated risk under comparable distance constraints (Section 5; see Figure 1). Taken together, this yields a reproducible pipeline for estimating exposure-adjusted crash risk at street and junction levels from measured cyclist volumes, and a safety-aware routing approach under a bounded detour constraint.

2. Data

We combine police-recorded bicycle crashes with measured cyclist exposure for the city of Berlin. Crash data are drawn from the Berlin subset of the German *Accident Atlas* (German Federal Statistical Office, 2025) and filtered for bicycle-related incidents. Exposure is obtained from a city-wide dataset of Strava-derived bicycle volumes aggregated at the street-segment level (Kaiser et al., 2025b). We further perform a consistency check between Strava-derived cyclist volumes and official bicycle counting stations (see Figure 2). The street network is represented as polyline segments with associated monthly cyclist counts. The dataset spans 2019–2023 and covers 4,335 street segments, 2,862 junctions, and 15,396 recorded bicycle crashes. At monthly resolution the data are sparse: in a typical month fewer than 5% of segments and about 3% of junctions record at least one crash.

verify the percentages

To enable network-scale analysis, all layers are harmonized to a common street-network topology and projected coordinate reference system. Crash locations are matched to segments using nearest-segment assignment. Junctions are defined as nodes where at least three segments meet; crashes within a fixed radius are assigned to the nearest junction, and junction exposure is computed from incident segments. Crashes and exposures are aggregated to monthly resolution, with segments and months of zero exposure dropped. To obtain stable risk estimates under sparse observations, monthly aggregates are pooled over the full study period and an Empirical Bayes approach is applied (Section 3). The resulting segment- and junction-level risk estimates serve as inputs to all routing analyses.

3. Methods

Empirical Bayes relative risk and uncertainty. For each month t , let $A_{s,t}$ and $E_{s,t}$ denote the number of police-

*Equal contribution. Correspondence to: Tobias Schnarr <tobias-marco.schnarr@student.uni-tuebingen.de>.

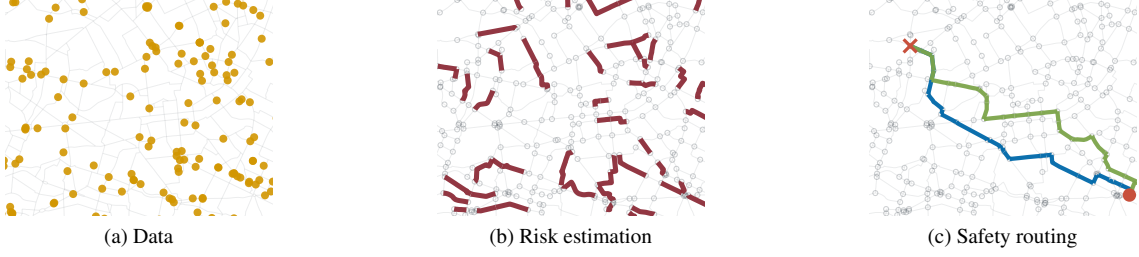


Figure 1. Safety-aware routing pipeline for the Berlin cycling network. Panels (a–c) are zoomed in for readability; see Section 3 for definitions and notation. (a) Police-recorded bicycle crashes in June 2021 (points) and street segments with measured cyclist exposure (lines). (b) Pooled segment-level relative crash risk estimated from all available data; high-risk segments in red correspond to values above the 90th percentile of relative risk; circles mark junctions ($\text{degree} \geq 3$). (c) Shortest path (blue) versus a safer alternative (green) selected to reduce cumulative relative route risk under a distance-detour constraint. Filled circle and cross denote origin and destination, respectively.

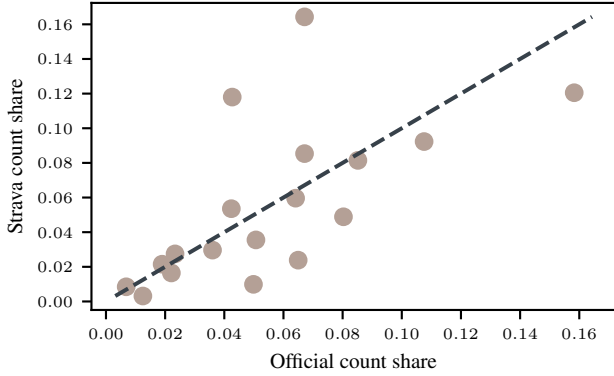


Figure 2. Consistency check between official bicycle counts and Strava-derived cyclist volumes at the street-segment level (2023). Points show segment-wise shares of total annual counts; the dashed line denotes equality between the two measures.

recorded bicycle crashes and measured cyclist exposure on street segment s . Junction crashes $A_{v,t}$ are defined as crashes within a fixed radius of junction v . Because a traversal typically contributes exposure to two incident segments, we approximate junction exposure by the half-sum of incident segment exposures,

$$E_{v,t} = \frac{1}{2} \sum_{s \in \mathcal{I}(v)} E_{s,t},$$

a common approach when turning movements are unavailable (Hakkert & Braimaister, 2002; Wang et al., 2020). For notational convenience, both street segments and junctions are indexed by a generic entity index i , with $A_{i,t}$ and $E_{i,t}$ denoting the corresponding crash and exposure quantities.

Under a no-special-risk baseline, monthly crash incidence is assumed proportional to exposure, yielding the expected

number of crashes

$$\hat{A}_{i,t} = A_{\cdot t} \frac{E_{i,t}}{E_{\cdot t}}, \quad A_{\cdot t} = \sum_i A_{i,t}, \quad E_{\cdot t} = \sum_i E_{i,t},$$

where sums are taken jointly over all segments and junctions, defining a shared baseline. Because routing requires a stable long-run risk surface, crashes and baseline expectations are aggregated over the full study period,

$$A_i = \sum_t A_{i,t}, \quad \hat{A}_i = \sum_t \hat{A}_{i,t},$$

and the raw relative risk is A_i / \hat{A}_i .

To stabilize estimation under sparsity, we introduce a latent relative-risk multiplier θ_i and model

$$A_i | \theta_i \sim \text{Poisson}(\hat{A}_i \theta_i), \quad \theta_i \sim \text{Gamma}(\alpha, \alpha),$$

where the Gamma prior (shape–rate) enforces $\mathbb{E}[\theta_i] = 1$ (Lord & Mannering, 2010). The shrinkage parameter α is estimated by method of moments (Morris, 1983). Under the Poisson–Gamma model,

$$\mathbb{E}[A_i] = \hat{A}_i \quad \text{and} \quad \text{Var}(A_i) = \hat{A}_i + \frac{\hat{A}_i^2}{\alpha}.$$

Equating empirical and theoretical second moments across entities yields

$$\hat{\alpha} = \frac{\sum_i \hat{A}_i^2}{\sum_i (A_i - \hat{A}_i)^2 - \sum_i \hat{A}_i}.$$

By conjugacy,

$$\theta_i | A_i, \hat{A}_i \sim \text{Gamma}(A_i + \alpha, \hat{A}_i + \alpha), \quad (1)$$

and the posterior mean

$$r_i = \mathbb{E}[\theta_i | A_i, \hat{A}_i] = \frac{A_i + \alpha}{\hat{A}_i + \alpha}$$

serves as the Empirical Bayes relative risk, with stronger shrinkage for entities with low expected counts (Hauer et al., 2002). Uncertainty is quantified using $(1 - \delta)$ credible intervals obtained from Gamma posterior quantiles.

Risk-weighted routing graph. Relative risk estimates are dimensionless and conditional on exposure. To obtain additive weights for routing, we rescale relative risk by the pooled baseline crash rate

$$\bar{\lambda} = \frac{A}{E}, \quad A = \sum_i A_i, \quad E = \sum_i E_i.$$

The resulting routing weight is

$$w_i = \bar{\lambda} r_i.$$

We construct an undirected graph $G = (V, E)$ from the street network. Nodes correspond to segment endpoints and edges to street segments with length ℓ_e . Each edge e corresponds to a segment s and inherits its routing weight $w_e = w_s$. Junction identifiers and weights are mapped to nodes via spatial snapping in a projected coordinate system, yielding a single risk-annotated network.

Safety-aware routing. We compare shortest-distance routes with alternatives that reduce estimated crash risk under a bounded detour. The length of a route P is

$$L(P) = \sum_{e \in P} \ell_e.$$

To account for segment- and junction-level risk, the risk contribution of edge $e = (u, v)$ is

$$\rho_e = w_e + \eta \frac{w_u + w_v}{2},$$

where w_u and w_v are junction routing weights (zero for non-junction nodes) and $\eta \geq 0$ controls the contribution of junction risk. These quantities form an *additive surrogate* for cumulative route risk.

For an origin–destination pair, the baseline route P_{dist} minimizes $L(P)$. The safety-aware route solves

$$\begin{aligned} P_{\text{safe}} &= \arg \min_P R(P) = \sum_{e \in P} \rho_e \\ \text{s.t. } L(P) &\leq (1 + \varepsilon) L(P_{\text{dist}}), \end{aligned} \tag{2}$$

where ε is the allowable relative detour (Ehrgott, 2005). We approximate this constraint via a weighted-sum sweep: for $\lambda \in \Lambda$,

$$P(\lambda) = \arg \min_P \sum_{e \in P} (\rho_e + \lambda \ell_e),$$

and select among feasible candidates the route minimizing $R(P)$. Shortest paths are computed with Dijkstra’s algorithm.

Evaluation metrics. For each origin–destination pair, we report the relative length increase

$$\Delta_L = \frac{L(P_{\text{safe}}) - L(P_{\text{dist}})}{L(P_{\text{dist}})}$$

and the relative risk reduction

$$\Delta_R = \frac{R(P_{\text{dist}}) - R(P_{\text{safe}})}{R(P_{\text{dist}})}.$$

Pairs with $R(P_{\text{dist}}) = 0$ are excluded from Δ_R due to the undefined denominator. These metrics quantify the trade-off between distance and exposure-adjusted crash risk under bounded detours.

4. Related work.

Prior work seeks to avoid conflating danger with demand by normalizing bicycle crashes by cyclist exposure (Lücken, 2018). City-scale studies show that exposure-normalized risk yields more informative spatial patterns than raw crash counts and that finer temporal resolution improves inference, though persistent under-reporting in police records remains a challenge (Uijtdewilligen et al., 2024). A central obstacle is obtaining reliable exposure: earlier work extrapolates city-wide volumes from sparse counters using learning-based models and multi-source features, while short-term measurement campaigns improve predictions at unseen locations (Kaiser et al., 2025a). More recent efforts instead rely on street-segment datasets of measured bicycle volumes, enabling safety analyses without explicit exposure modeling (Kaiser et al., 2025b). At the network level, risk is typically defined as crashes per unit exposure on links, with attention to spatial snapping, assignment of incidents to intersections, and integration of safety metrics into routing under convenience constraints (Wage et al., 2022). Intersection safety is repeatedly emphasized, with strong crash concentrations at junctions and the need to control for exposure when comparing locations or infrastructure types (Medeiros et al., 2021).

In contrast, we combine measured segment-level exposure with joint segment–junction risk estimation and propagate these risks into safety-aware routing.

this sentence can be dropped if space is an issue

5. Results

One of the major outcomes of this work is the estimation of the risk to have gotten injured in a bike accident while driving on a streetsegment. This distribution of those calculated risks is displayed in .

To evaluate the routing algorithm, we sample $n = 1000$ origin–destination pairs uniformly at random and compare shortest-distance routes with safety-aware alternatives (Natera Orozco et al., 2020).



Figure 3. Closer investigation on Junction 2482 Colors in (a) and (b) (—) represent the log-scaled risk, ranging from blue (low risk) to red (high risk). As one example the junction on Hermann-Hesse-Straße and Heinrich-Mann-Straße was observed further. There were 22 Accidents as displayed in the map. The recorded accidents involved a second vehicle, predominantly cars (20 cases), with only two involving other vehicle types. Most accidents were caused by vehicles turning into or crossing a road (20), while only a few resulted from turning off the road (2). Looking at Google Street view (Google, 2025) this seems to make sense since the car lane is crossing the bicycle lane in this place.

Table 1. Distance–risk trade-off under bounded detours for different junction-risk weights η . Values are aggregated over all origin–destination pairs. Medians are reported with interquartile ranges in parentheses. $P(\Delta_R > 0)$ is reported in percent.

η	ε	Med. Δ_L	Med. Δ_R	$P(\Delta_R > 0)$
0.0	0.05	0.009 (0.026)	0.246 (0.451)	76.1
	0.10	0.025 (0.042)	0.377 (0.388)	86.0
	0.20	0.038 (0.072)	0.425 (0.353)	90.6
0.5	0.05	0.008 (0.026)	0.208 (0.401)	75.3
	0.10	0.026 (0.046)	0.331 (0.370)	86.4
	0.20	0.047 (0.089)	0.404 (0.323)	92.0
1.0	0.05	0.008 (0.026)	0.185 (0.363)	75.9
	0.10	0.028 (0.047)	0.305 (0.345)	86.3
	0.20	0.050 (0.086)	0.378 (0.318)	91.8

Table 1 summarizes the trade-off between route length and exposure-adjusted crash risk under bounded detours. Safety-aware routing identifies feasible alternatives for all origin–destination pairs across detour budgets and junction-risk weights.

Allowing a 10% detour reduces exposure-adjusted crash risk by 31–38% in median, with over 86% of routes achieving a risk reduction for all values of the junction-risk weight. Larger detours further increase these gains, reaching median reductions of 38–43% at $\varepsilon = 0.20$, while even small detours ($\varepsilon = 0.05$) yield measurable reductions of 18–25%. Across all detour budgets, increasing η is associated with lower median risk reductions.

6. Discussion and Conclusion

Our results indicate that substantial reductions in exposure-adjusted crash risk can be achieved with relatively small

increases in route length. While higher junction-risk weights reduce the magnitude of the estimated risk reduction, the distance–risk trade-off persists across all configurations, with absolute gains depending on the chosen weighting.

Overall, allowing a 10% increase in route length yields median exposure-adjusted risk reductions of 31–38% for the majority of routes, demonstrating that safety-aware routing can effectively trade modest detours for meaningful safety improvements.

We provide implementation details, hyperparameters, and supplementary material, available at https://github.com/ytobiaz/data_literacy.

Contribution Statement

Explain here, in one sentence per person, what each group member contributed. For example, you could write: Max Mustermann collected and prepared data. Gabi Musterfrau and John Doe performed the data analysis. Jane Doe produced visualizations. All authors will jointly wrote the text of the report. Note that you, as a group, a collectively responsible for the report. Your contributions should be roughly equal in amount and difficulty.

References

- Ehrgott, M. *Multicriteria Optimization*, volume 491 of *Lecture Notes in Economics and Mathematical Systems*. Springer, Berlin, Heidelberg, 2005. ISBN 978-3-540-21398-7. URL <https://doi.org/10.1007/3-540-27659-9>.
- German Federal Statistical Office. Accident Atlas, 2025. URL <https://unfallatlas.statistikportal.de>.
- Google. Google Street View: Junction Heinrich-Mann-Straße/Hermann-Hesse-Straße Berlin, 2025. URL <https://maps.app.goo.gl/pxxqfSwW8Rbtu6AZ8>.
- Hakkert, A. S. and Braimaister, L. The uses of exposure and risk in road safety studies. Technical Report R-2002-12, SWOV Institute for Road Safety Research, Leidschendam, The Netherlands, 2002. URL <http://www.swov.nl/rapport/R-2002-12.pdf>.
- Hauer, E., Harwood, D. W., Council, F. M., and Griffith, M. S. Estimating safety by the empirical bayes method: A tutorial. *Transportation Research Record: Journal of the Transportation Research Board*, 1784(1):126–131, 2002. ISSN 2169-4052. doi: 10.3141/1784-16. URL <https://dx.doi.org/10.3141/1784-16>.
- Kaiser, S. K. Data from: Spatio-temporal graph neural network for urban spaces: Interpolating citywide traffic volume, 2025. URL <https://doi.org/10.5281/zenodo.15332147>.
- Kaiser, S. K., Klein, N., and Kaack, L. H. From counting stations to city-wide estimates: data-driven bicycle volume extrapolation. *Environmental Data Science*, 4:e13, 2025a. doi: 10.1017/eds.2025.5.
- Kaiser, S. K., Rodrigues, F., Azevedo, C. L., and Kaack, L. H. Spatio-temporal graph neural network for urban spaces: Interpolating citywide traffic volume, 2025b. URL <https://arxiv.org/abs/2505.06292>.
- Lord, D. and Mannering, F. The statistical analysis of crash-frequency data: A review and assessment of methodological alternatives. *Transportation Research Part A: Policy and Practice*, 44(5):291–305, 2010. ISSN 0965-8564. doi: 10.1016/j.tra.2010.02.001. URL <http://dx.doi.org/10.1016/j.tra.2010.02.001>.
- Lücken, L. On the variation of the crash risk with the total number of bicyclists. *European Transport Research Review*, 10(2):33, 2018. doi: 10.1186/s12544-018-0305-9. URL <https://doi.org/10.1186/s12544-018-0305-9>.
- Medeiros, R. M., Bojic, I., and Jammot-Paillet, Q. Spatiotemporal variation in bicycle road crashes and traffic volume in berlin: Implications for future research, planning, and network design. *Future Transportation*, 1(3):686–706, 2021. ISSN 2673-7590. doi: 10.3390/futuretransp1030037. URL <https://www.mdpi.com/2673-7590/1/3/37>.
- Morris, C. N. Parametric empirical bayes inference: Theory and applications. *Journal of the American Statistical Association*, 78(381):47–55, 1983. ISSN 1537-274X. doi: 10.1080/01621459.1983.10477920. URL <http://dx.doi.org/10.1080/01621459.1983.10477920>.
- Natera Orozco, L. G., Battiston, F., Iñiguez, G., and Szell, M. Data-driven strategies for optimal bicycle network growth. *Royal Society Open Science*, 7(12):201130, 2020. ISSN 2054-5703. doi: 10.1098/rsos.201130. URL <http://dx.doi.org/10.1098/rsos.201130>.
- Uijtdewilligen, T., Ulak, M. B., Wijlhuizen, G. J., Blijleveld, F., Geurs, K. T., and Dijkstra, A. Examining the crash risk factors associated with cycling by considering spatial and temporal disaggregation of exposure: Findings from four dutch cities. *Journal of Transportation Safety & Security*, 16(9):945–971, 2024. doi: 10.1080/19439962.2023.2273547. URL <https://doi.org/10.1080/19439962.2023.2273547>.
- Wage, O., Bienzeisler, L., and Sester, M. Risk analysis of cycling accidents using a traffic demand model. *The International Archives of the Photogrammetry, Remote Sensing and Spatial Information Sciences*, XLIII-B4-2022:427–434, 2022. doi: 10.5194/isprs-archives-XLIII-B4-2022-427-2022. URL <https://isprs-archives.copernicus.org/articles/XLIII-B4-2022/427/2022/>.
- Wang, K., Zhao, S., and Jackson, E. Investigating exposure measures and functional forms in urban and suburban intersection safety performance functions using generalized negative binomial - p model. *Accident Analysis and Prevention*, 165:106275, 2023. doi: 10.1016/j.aap.2023.106275.

Analysis & Prevention, 148:105838, 2020. ISSN 0001-4575. doi: <https://doi.org/10.1016/j.aap.2020.105838>.
URL <https://www.sciencedirect.com/science/article/pii/S0001457520316584>.